Stellar Populations in the Milky Way and Beyond
Proceedings IAU Symposium No. 395, 2026
J. Meléndez, C. Chiappini, R. Schiavon & M. Trevisan, eds.
doi:10.1017/S1743921325001681

Initial mass function of the Galactic bulge from binary microlensing events

Raphael A. P. Oliveira and OGLE Team

Astronomical Observatory, University of Warsaw, Al. Ujazdowskie 4, 00-478 Warszawa, Poland

Abstract. The initial mass function of the Galactic bulge can be obtained from Hubble Space Telescope luminosity functions if the statistics of binary stellar systems is well constrained. Such statistics can be estimated using gravitational microlensing effect, which is sensitive to the masses of lensing objects. Current microlensing surveys are sensitive to microlensing signals produced by low-mass stars in the bulge. We propose to search for and analyze microlensing events containing binary lens or binary source in light curves of large microlensing surveys, including low-mass, unresolved binaries. We implemented a fully-automated approach in the search and characterization of new and previously identified events. With the consideration of detection efficiency, the large statistics of binaries gives constraints for the binary fraction and mass-ratio distribution. In this work, methods and results for some events with well-separated bumps are presented.

Keywords. gravitational lensing: micro, Galaxy: bulge, stars: mass function

1. Introduction

The initial mass function (IMF) of a system dictates the relative number of stars as a function of mass at the moment of birth, serving as a crucial ingredient to quantify the star formation and evolution processes. The IMF is relatively well determined for the Solar neighborhood and star clusters, following a power law $\mathrm{d}N/\mathrm{d}M \propto m^{-\alpha}$ with $\alpha = -2.35$ down to $\sim 0.5 M_{\odot}$ (Salpeter 1955), and a log-normal or shallower power law with $\alpha = -1.3$ below (Kroupa *et al.* 2001; Chabrier 2003). Several works tested the IMF universality for farther systems, e.g., Magellanic Clouds, ultra-faint dwarf galaxies and early-type galaxies (Bastian et al. 2010).

For the Galactic bulge, precise luminosity functions from the Hubble Space Telescope lack tighter constraints on binary fraction and mass ratio distribution to derive the IMF. For example, Calamida *et al.* (2015) derived the IMF down to $0.15\,M_{\odot}$ as two power laws with a break at $0.56\,M_{\odot}$, with different slopes depending on the assumed binary fraction and mass ratio. The derived IMFs show a good agreement above the mass break but a larger spread for low-mass stars, with slopes between -0.89 and -1.51 for binary fractions of 0% and 100%, respectively. Knowing the IMF down to the low masses is key to constrain the star formation history and chemical enrichment models of the Galaxy, and extrapolate to other galaxies.

Gravitational microlensing events take place when the light of a background star is magnified by a foreground, massive object passing at a close angle. The intensity of the lensing effect depends on the lens mass, not brightness, and occurs more frequently in crowded fields. It makes microlensing the best option to assess the bulge IMF down to low-mass stars, including unresolved binaries. In this work, we present an automated

© The Author(s), 2026. Published by Cambridge University Press on behalf of The International Astronomical Union.

https://doi.org/10.1017/S1743921325001681 Published online by Cambridge University Press

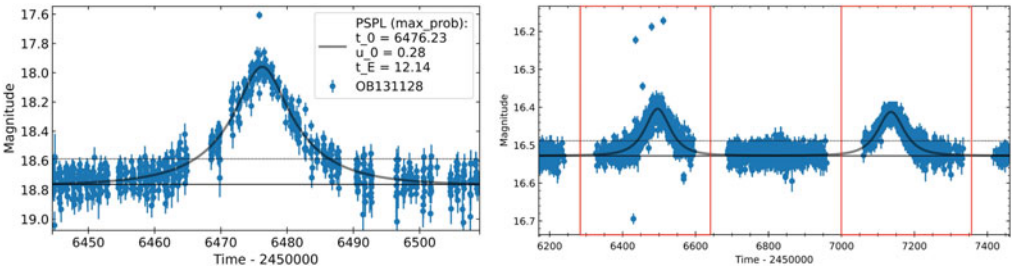


Figure 1. Examples retrieved by the detection algorithm. The horizontal solid and dashed lines represent the baseline flux and 3σ-level, respectively. *(Left:)* Event with a single bump, which was detected as dozens of datapoints more than 3σ above the baseline flux. The PSPL model parameters are explained in Section 3. *(Right:)* Event with two bumps, for which the two windows (red rectangles) were necessary in order to get a more precise baseline flux.

approach to select binary events and obtain the best fitting models, limited initially to those with well-separated bumps.

2. Data and automated detection of binary events

The Optical Gravitational Lensing Experiment (OGLE) survey is one of the largest long-term photometric surveys, starting in 1992 and on the fourth phase since 2010. It was designed to search for dark matter with microlensing phenomena and contains the largest collection of variable stars. It uses the 1.3 m Warsaw telescope, at the Las Campanas Observatory, equipped with a mosaic camera of 32 CCDs of field of view 1.4 $\deg^2$ (Udalski *et al.* 2015).

The timescale distribution of a large sample of microlensing events is often used to measure the mass distribution of lenses and their mass function (e.g., Sumi *et al.* 2011; Wyrzykowski *et al.* 2015; Mróz *et al.* 2019). Mróz *et al.* (2019) analysed 121 OGLE fields towards the bulge, detecting 8000 microlensing events and producing maps of event rate and optical depth. They applied an automated algorithm for event detection, based on finding light curves at least three datapoints 3σ above the baseline flux (obtained removing datapoints close to the bump). This group of algorithms, however, usually reject binary events, by applying cuts in goodness-of-fit of point-source/point-lens models (PSPL) or limiting the number of bumps to one.

In the present work, we analyse 400 million sources in the same 121 OGLE fields, in order to search for binary microlensing events with well-separated bumps. Nine fields contain high-cadence data, with about 15000 epochs between 2010 and 2017, whereas the others have lower cadence with less than 3000 epochs. The algorithm from Mróz *et al.* (2019) was adopted with some optimizations for binaries: slope correction to the baseline, assumption of a second window to get the baseline flux, bump removals to check for additional bumps, and tighter thresholds. Figure 1 provides two examples of event detection: one single-peaked event along with the PSPL fit and a binary, double-peaked event using the two windows.

A sample of 29 "benchmark" events was obtained from visual inspection of a selection of OGLE alerts, all of them containing two clear bumps, with the datapoints in between reaching the baseline flux. The algorithms were adapted and optimized in order to detect all benchmark events. Compared to Mróz *et al.* (2019, their Table 2), we applied more strict thresholds, in order to exclude noisy light curves, photometric artifacts and reduce the false positives count. Oliveira et al. (in preparation) details the algorithm and number of detections.

https://doi.org/10.1017/S1743921325001681 Published online by Cambridge University Press

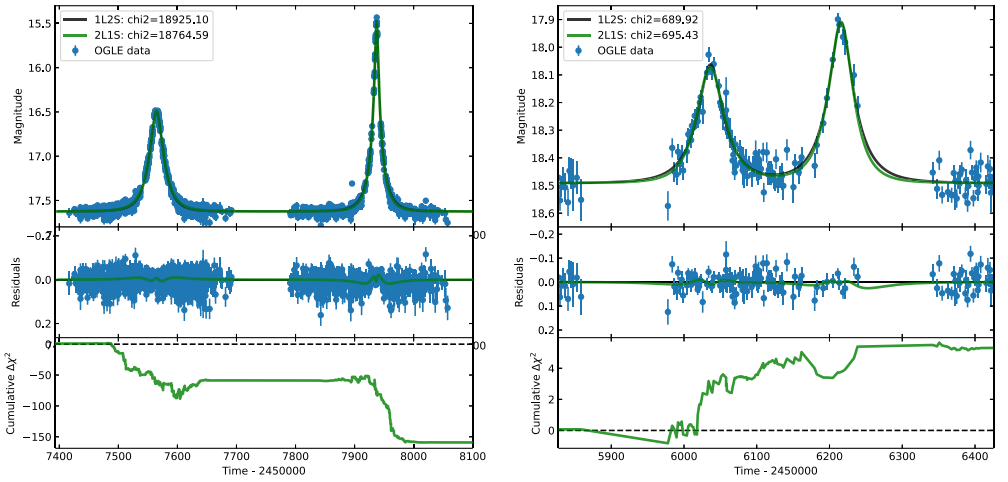


Figure 2. Results obtained for two benchmark clusters, with a comparison between the 1L2S and 2L1S models. *(Left:)* Binary event BLG505.03.213693, with the 2L1S model more favored in both bumps, by a $\Delta\chi^2$ of ~ 150. *(Right:)* Binary event BLG510.11.45341, with the 1L2S model more favored by a $\Delta\chi^2$ of ~ 4. The derived parameters and corner plots are available in Oliveira et al. (in prep.).

3. Model fitting and results

In a microlensing PSPL event, the point-lens magnifies the observed flux according to:

$$A = \frac{u^2+2}{u\sqrt{u^2+4}} \text{ , where } u(t) = \sqrt{u_0^2 + \left(\frac{t-t_0}{t_\mathrm{E}}\right)^2}. \quad (1)$$

The parameters t_0, u_0 and t_E correspond to the time of closest approach, impact parameter and Einstein timescale. The presence of a binary companion changes the light curve significantly. If the source is a binary star (1L2S), it consists of a superposition of two PSPL events of same t_E if the source orbital motion is ignored, with parameters: $t_{0,1}$, $u_{0,1}$, $t_{0,2}$, $u_{0,2}$, and t_E. If the lens is a binary star (2L1S), fifth-order complex polynomials are solved and complex caustic patterns (infinite magnification) may appear, with parameters: t_0, u_0, t_E, mass ratio q, separation s, and source trajectory angle α. However, in the cases considered in this work (separated bumps without caustics), the two models are very similar.

The model fitting was carried out with the `MulensModel` code (Poleski & Yee 2019), which allows modelling of both binary source and binary lens, χ^2 evaluation and Bayesian inference. An algorithm was implemented to optimize the 1L2S fitting: detecting the time instant of maximum magnitude between the two bumps, divide the data into two groups and obtain two separate, independent PSPL fits. The derived PSPL parameters are used as initial guesses, both for the final 1L2S and 2L1S fitting. Both fits are obtained with MCMC sampling (Foreman-Mackey *et al.* 2013), with the 2L1S one using the `point_source` method.

Figure 2 presents the results for two benchmark clusters, comparing between the 1L2S and 2L1S models. The lower panels, with the cumulative χ^2 evaluated at each point, make clear which model is favored in each case. For BLG510.11.45341, the difference in cumulative χ^2 was much smaller and required the evaluation of the evidence from nested sampling (UltraNest; Buchner 2021) and the amount of negative blending flux.

https://doi.org/10.1017/S1743921325001681 Published online by Cambridge University Press

Acknowledgments

The author salutes this conference in honor of the brilliant scientist Prof. Beatriz Barbuy, who has been fundamental to his scientific career. This research was funded in part by the National Science Center, Poland, grant Sonata Bis 2021/42/E/ST9/00038 to Radoslaw Poleski.

References

Bastian, N., Covey, K. R., & Meyer, M. R. 2010, ARA&A, 48, 339.
Buchner, J. 2021, The Journal of Open Source Software, 6, 3001.
Calamida, A., Sahu, K. C., Casertano, S.*et al.* 2015, ApJ, 810, 8.
Chabrier, G. 2003, PASP, 115, 763.
Foreman-Mackey, D., Hogg, D. W., Lang, D., Goodman, J. 2013, PASP, 125, 306.
Kroupa, P. 2001, MNRAS, 322, 231.
Mróz, P., Udalski, A., Skowron, J.*et al.* 2019, ApJS, 244, 29.
Poleski, R., Yee, J. C. 2019, Astronomy and Computing, 26, 35.
Salpeter, E. E. 1955, ApJ, 121, 161.
Sumi, T., Kamiya, K., Bennett, D. P.*et al.* 2011, Nature, 473, 349.
Udalski, A., Szymański, M. K., Szymański, G. 2015, Acta Astron., 65, 1.
Wyrzykowski, Ł, Rynkiewicz, A. E., Skowron, J.*et al.* 2015, ApJS, 216, 12.

https://doi.org/10.1017/S1743921325001681 Published online by Cambridge University Press

https://doi.org/10.1017/S1743921325001681 Published online by Cambridge University Press